LABORATORY INVESTIGATION OF IMPACT FORCES

A. FÜHRBÖTER

Franzius-Institut für Grund-und Wasserbau der Technische Universität Hannover
Hannover, Germany

Contents:

Summary:

A special impact generator was constructed in order to produce water impacts with velocities which are not available in scale models with waves.

The water impact was generated by a jet suddenly striking upon a measuring area.

Even under same conditions of impact, stochastic scattering of the peak pressures was observed; but for all test series the distribution of frequencies of the pressures was found to be normal-logarithmic.

The generated shock pressures by an impact velocity v came higher than 10 times the maximum pressure of steady flow of equal velocity v; but they were lower than 10 % of the water hammer pressure $\varrho \cdot v \cdot c$.

Even by a thin sheet of water on the measuring area the shock pressures were damped nearly completely.

Considerations about the effect of air content in connection with the effects of expansion show that shock pressures can be explained by a damping of water hammer pressure by a small air content. Some evaluations of the test material are given to this point.

1. INTRODUCTION

Most of all experimental investigations on the problems of shock pressures generated by wave impact have been done in model wave channels.

The advantage of these test arrangements is, that the connection between the wave characteristics and the impact condition can be studied directly. On the other side, it is not possible to control the impact conditions systematically; especially the velocity of the impact is limited by the size of the wave channels, for waves up to .5 m high the impact velocities only range between 1 and 2 m/sec.

Furthermore, it is well known after the comprehensive study by DENNY (3) that impact pressures only can be described by stochastic laws. Using a wave channel, it is only possible to measure the superposition of wave and impact statistics. Already in the classical work by BAGNOLD (2) he noted how sensitively the appearance of impact forces changed with very small differences in the wave generation.

In order to seperate between wave conditions and the dynamics of impact, it was felt necessary to construct a special impact generator. This impact generator should simulate the prototype conditions as nearly as possible.

Shock pressures by impact occur by a sudden stopping of a moving mass of water by a rigid wall. This process can be reconstructed in a laboratory by a jet which is deflected in a very short time upon a measuring area representing the rigid wall.

The present paper deals with such special tests with an impact generator. It is of interest that GAILLARD (5) as early as 1904 described experiments with a similar impact generator. His results, however, were, that by an impacting mass of water with the velocity v no higher pressures could be measured than by a steady flow of same velocity. The reason was that the spring pressure meters used by him could not indicate the short-time rise of pressure which is characteristic for all shock pressures; the lack of electronic devices was responsible for this result.

2. THEORETICAL CONSIDERATION

Taking into account only the elasticity of water (by the density ϱ and the velocity of sound c in pure water), von KARMAN (7) gave the simple solution for maximum pressure during an impact

$$p_{max} = \varrho \cdot v \cdot c \quad \ldots\ldots\ldots\ldots\ldots\ldots\ldots\ldots\ldots\ldots (1)$$

BAGNOLD (2) first showed the high influence of entrapped air in the contact area between water and the rigid wall. The air in this contact area may occur in form of one or more cushions or bubbles; its influence on elasticity always can be reproduced by an average thickness D of a thin layer of air of equal volume.

For atmospheric pressure, the elasticity of water E stands in relation to the elasticity of air E_a like

$$\frac{E}{E_a} = 15500 \quad \ldots\ldots\ldots\ldots\ldots\ldots\ldots\ldots\ldots\ldots (2)$$

From this it can bee seen that the elasticity of the structure or of the wall in most cases can be neglected. Even a very thin layer of air gives a considerable damping to the pressure of impact.

Contrary to the phenomenon of water hammer effects in pipes, a free jet of water has no fixed boundaries on the sides. Therefore free expansion can take place at the circumference U of the impact area A; air entrainment and free expansion together provide shock pressures to rise till the magnitude of water hammer pressures.

In Fig. 1, the moment of impact of a free nappe of water is shown schematically for the case of a plane parallel front of the nappe before impact.

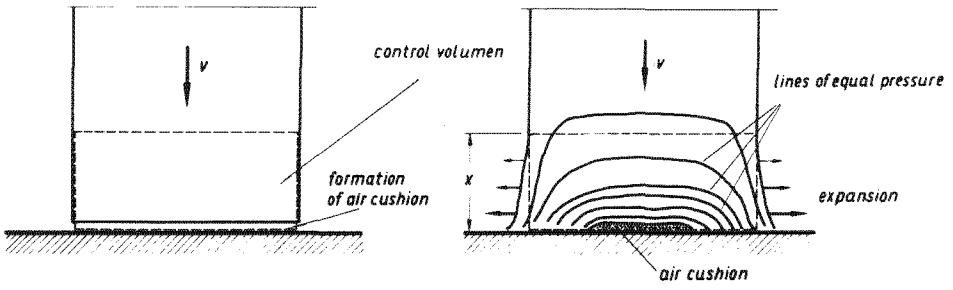

Fig. 1. Air entrairment and expansion during impact

With application of the law of continuity for each time element dt for the control volume in Fig. 1, it can be written (see also (4)).

$$A \cdot v \cdot dt = \left(\frac{A \cdot D}{E_a(t)} + \frac{A \cdot x(t)}{E}\right) dp + A_e(t) \cdot v_e \cdot dt \quad \ldots\ldots\ldots\ldots\ldots\ldots \quad (3)$$

(inflow) (compression of air and water) (outflow by expansion)

Here A is the area and v is the velocity of impact, D the representive thickness of the air cushion, $E_a(t)$ the adiabatic elasticity of the air corresponding to pressure and time, E the constant elasticity of water, x the unknown length of water in axis of the nappe compressed by dp; $A_e(t)$ the (average) area of expansion with the (average) outflow velocity v_e due to expansion.

From momentum equation for the direction parallel to the wall a relation between the expansion velocity v_e and the pressure p can be given by

$$K = p \cdot A_e = \varrho \cdot Q_e \cdot v_e = \varrho \cdot A_e \cdot v_e^2 \quad \text{or}$$

$$v_e = \sqrt{p/\varrho} \quad \ldots\ldots\ldots\ldots\ldots\ldots\ldots\ldots \quad (4)$$

It shall be mentioned that, because of the nonuniform distribution of pressure p over the impact area A and the expansion velocity v_e over the expansion area A_e, equation (4) can give only an approximation for the average values.

Introducing equation (4) in equation (3), there is a differential equation for p(t):

$$A \cdot v \cdot dt = \left(\frac{A \cdot D}{E_a(t)} + \frac{A \cdot x(t)}{E}\right) dp + A_e(t) \cdot \sqrt{p/\varrho} \cdot dt \quad \ldots\ldots\ldots \quad (5)$$

(inflow) (compression of air and water) (outflow by expansion)

A complete solution is not possible because of the many unknown variables; this complete solution, however, is not necessary when only the peak pressure p_{max} is desired; p_{max} is the maximum of p(t) during impact and is given by the condition

$$\frac{dp}{dt} = 0$$

which gives with equation (5) the simple relation

$$A \cdot v = A_e \cdot \sqrt{p_{max}/\varrho} \quad \ldots\ldots\ldots\ldots\ldots\ldots\ldots\ldots \quad (6)$$

(inflow)(outflow by expansion)

For the moment of maximum pressure p_{max} during impact, inflow in the control volume is equal to outflow on the sides by expansion. Before maximum pressure, the outflow is lower than the inflow; after maximum pressure, outflow becomes higher than inflow (4).

Equation (6) can be solved for p_{max} and gives

$$p_{max} = \varrho \cdot v^2 \cdot \left(\frac{A}{A_e}\right)^2 \quad \ldots\ldots\ldots\ldots\ldots\ldots\ldots \quad (6)$$

For $A_e(t)$ can be written $A_e(t)=U \cdot x(t)$ and for the time $p(t)=p_{max}$ $A_e = U \cdot x$; $A/U = R$ is the hydraulic radius of the impact area. So equation (6) becomes

$$p_{max} = \varrho \cdot v^2 \cdot \left(\frac{R}{x}\right)^2 \quad \ldots\ldots\ldots\ldots\ldots\ldots\ldots \quad (7)$$

From the cross section of the impinging nappe, R is known; the only unknown variable in equation (7) is the length x, the length on which expansion takes place according to Fig. 1.

In equation (7) the thickness D of the air cushion does not directly appear. Considering the pressure rise between p = 0 (beginning of impact) and p = p_{max}, it can be shown easily that there is a close connection between the length of the expanding area and the thickness of the air cushion in a manner, that x increases with increasing D. For a higher air cushion, the pressure rise is lower than for a small one; therefore a greater area for the expansion effect can be built up which makes x increase.

Stochastic effects are introduced by the variables x and R, where x is mostly connected with the accidental air content in the contact area, R with irregularities in the face of the impinging nappe.

3. EXPERIMENTAL RESULTS

On Fig. 2, the experimental equipment can be seen, which

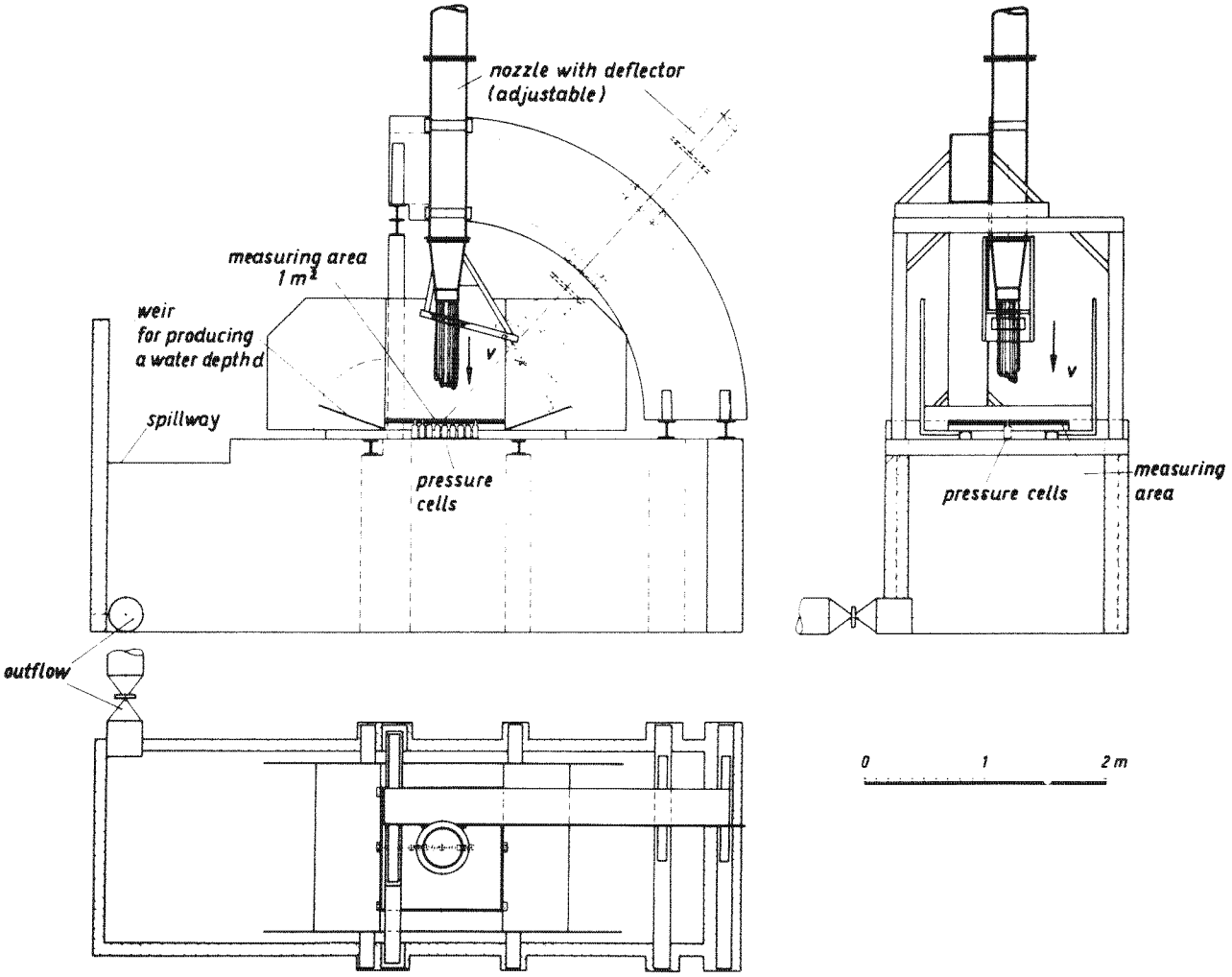

Fig. 2. Impact generator in the FRANZIUS-INSTITUT

was used to generate shock pressures by impact. The jet (diameter 200 mm) with the deflector mechanism for sudden opening was adjustable to any angle α between the jet axis and the measurement area, a strong plane steel plate with 8 electronic pressure cells in distances of 50 mm; the electronic equipments were selected so that single processes of only .001 sec and less could be recorded without damping (4).

For the front of the nappe, not only the jet angle α is of importance, but also the front angle ß which is formed by the short but not infinite short time of opening the deflector gate;

Fig. 3 shows these two angles at the face of the nappe.

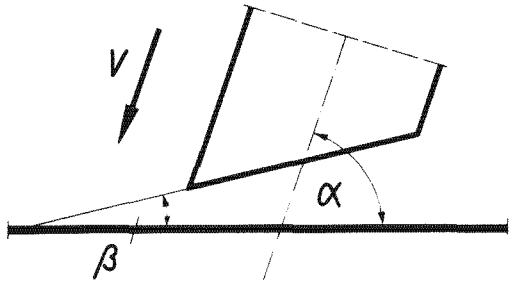

Fig. 3. Jet angle α and front angle ß

For a constant velocity

$$v = 8.3 \text{ m/sec}$$

(this would correspond to the impact velocity of a wave about 3 m high) a series of 6 x 100 tests were carried out for different jet and front angles; the results are summarized in the table on page 8 and in Figs. 4 to 9 on the following pages.

Each Fig. 4 to 9 shows a series of 100 tests; from the 8 pressure records on the measuring area the highest pressure p_{max} was taken for the evaluation. Mostly the pressures were distributed uniformly over the measuring area and did not differ very much from one to another; only to the borders of the nappe also the peak pressures became lower.

If t_1 is the time for the pressure rise from zero to p_{max} and t_2 the time for the pressure drop from p_{max} to p_s (maximum pressure of the jet with steady flow with v), the records showed

t_1 between .001 and .002 secs
t_2 between .002 and .004 secs

according to a complete duration of shock pressure t_s

t_s between .003 and .006 secs,

the longer durations belonging to low, the shorter to high pressure peaks as already shown by BAGNOLD (2).

The maximum pressure p_s on an area under a jet of steady flow with the velocity v is

$$p_s = \varrho \cdot \frac{v^2}{2} \quad \ldots\ldots\ldots\ldots\ldots\ldots\ldots\ldots\ldots \quad (8)$$

and for v = const. = 8.3 m/sec.

$$p_s = 3.5 \text{ m (water column)}$$

for all angles of approach α. The results show that the highest

p_{max} m		$\alpha = 90°$ $\beta = +33{,}8°$	$\alpha = 82{,}5°$ $\beta = +23{,}7°$	$\alpha = 75°$ $\beta = +18°$	$\alpha = 60°$ $\beta = +3{,}6°$	$\alpha = 45°$ $\beta = -17{,}5°$	$\alpha = 30°$ $\beta = -35°$
from	to	Number	Number	Number	Number	Number	Number
1,0	1,9						
2,0	2,9						4
3,0	3,9						2
4,0	4,9						4
5,0	5,9						8
6,0	6,9						13
7,0	7,9	1					3
8,0	8,9	4				1	13
9,0	9,9	4	2	2	3	3	12
10,0	10,9	15	6	2	1	4	3
11,0	11,9	13	4	2	1	8	8
12,0	12,9	14	4	9	2	6	5
13,0	13,9	7	13	11	5	7	8
14,0	14,9	5	8	2	8	6	3
15,0	15,9	7	8	11	10	14	1
16,0	16,9	7	10	13	8	8	4
17,0	17,9	6	6	5	8	6	4
18,0	18,9	3	8	7	13	6	1
19,0	19,9	3	5	9	4	7	1
20,0	20,9	2	4	5	5	4	1
21,0	21,9		2	5	7	3	
22,0	22,9	3	2	5	5	6	1
23,0	23,9	2	3	4	4	1	
24,0	24,9	2	3	2	3	1	
25,0	25,9		1	2	2	4	
26,0	26,9	1	1	1	2		
27,0	27,9		2	1	3		1
28,0	28,9				1	1	
29,0	29,9		2	1	1	1	
30,0	30,9		2		1		
31,0	31,9	1		1	1		
32,0	32,9					1	
33,0	33,9		1				
34,0	34,9					1	
35,0	35,9						
36,0	36,9				1	1	
37,0	37,9						
38,0	38,9		2				
39,0	39,9				1		
40,0	40,9		1				
41,0	41,9						
42,0	42,9						
43,0	43,9						
44,0	44,9						
45,0	45,9						
46,0	46,9						
47,0	47,9						
48,0	48,9						
49,0	49,9						
Σ =		100	100	100	100	100	100

Table: Frequencies of maximum pressures p_{max}

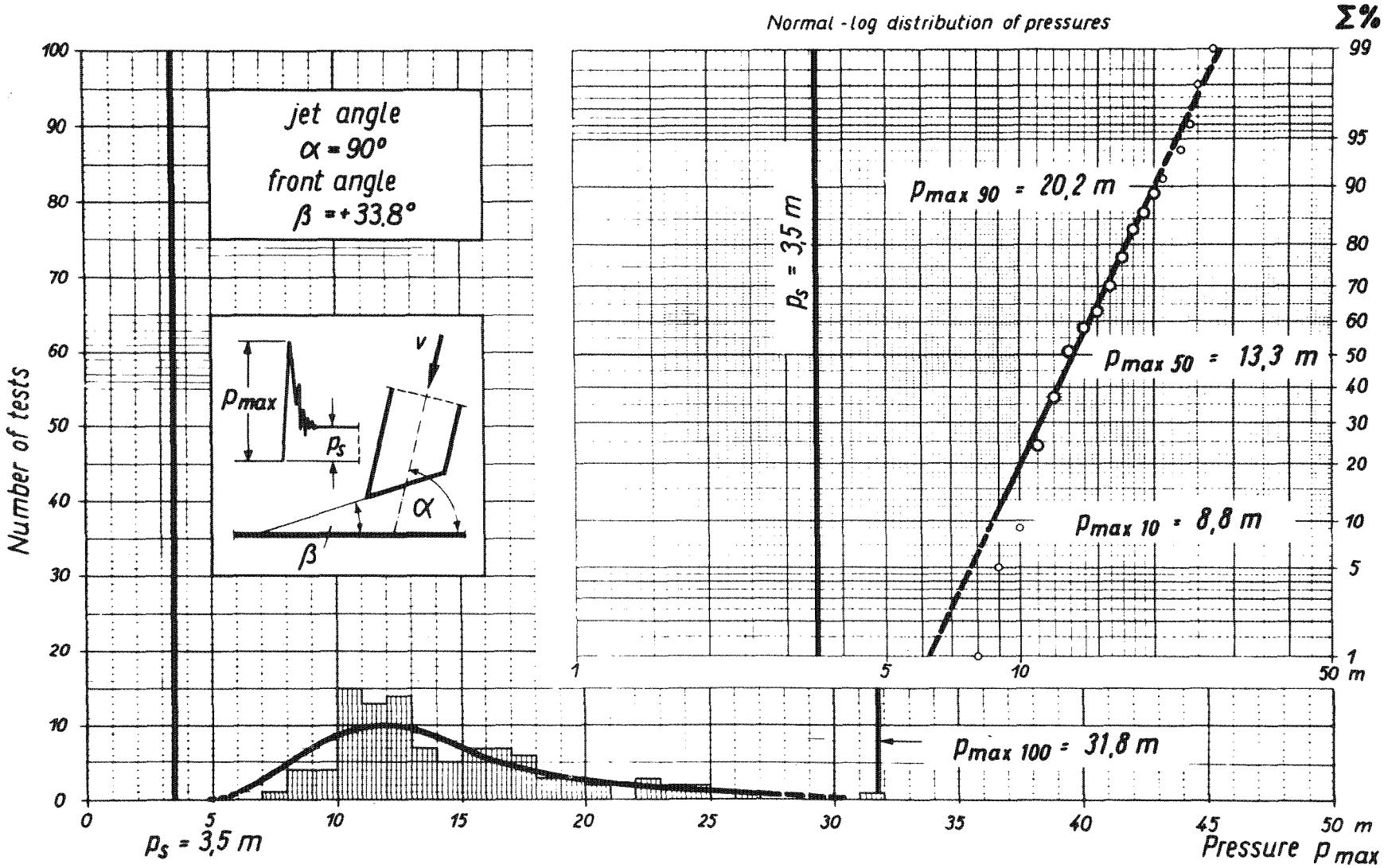

Fig. 4. Frequencies of maximum pressures p_{max}

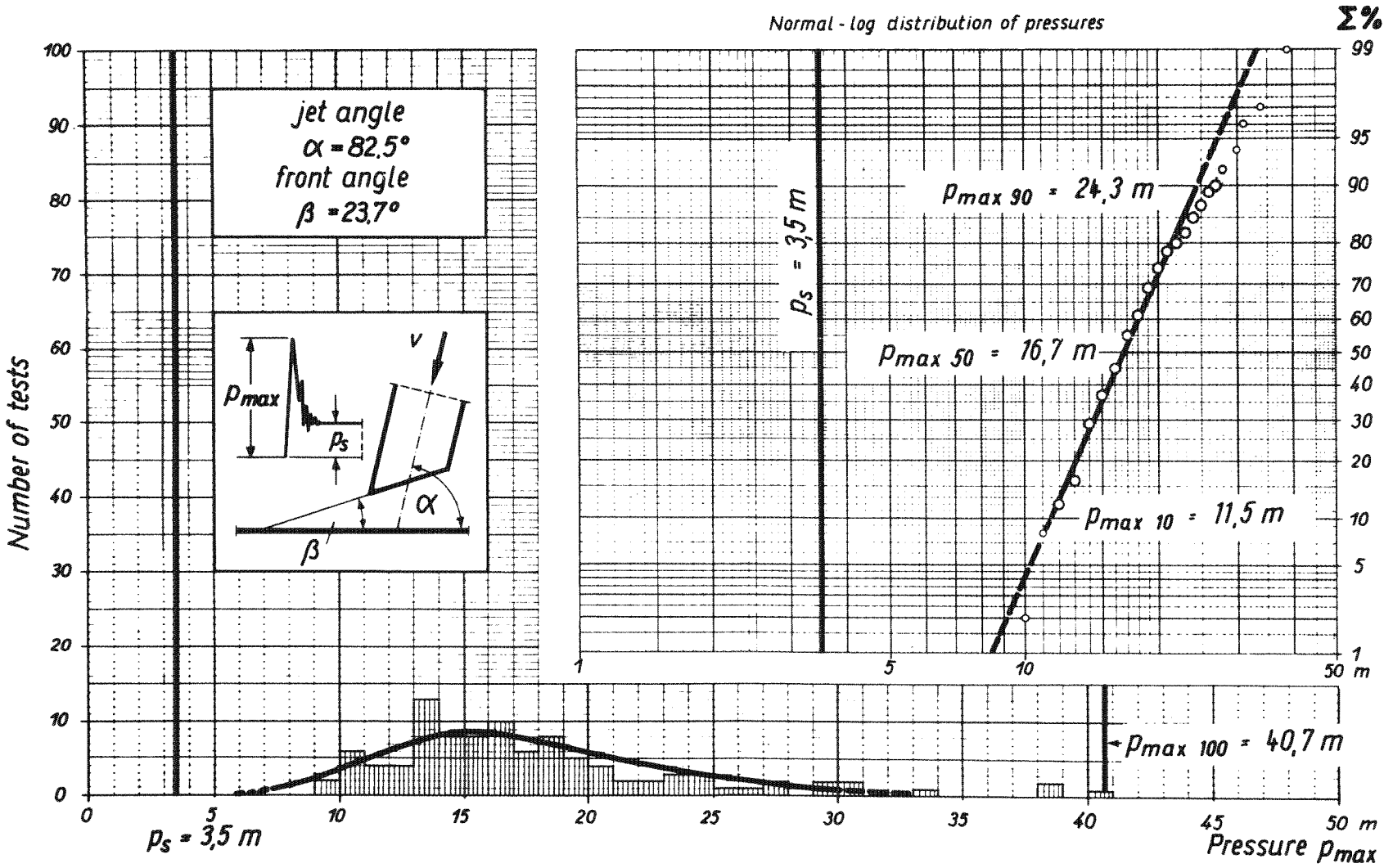

Fig. 5. Frequencies of maximum pressures p_{max}

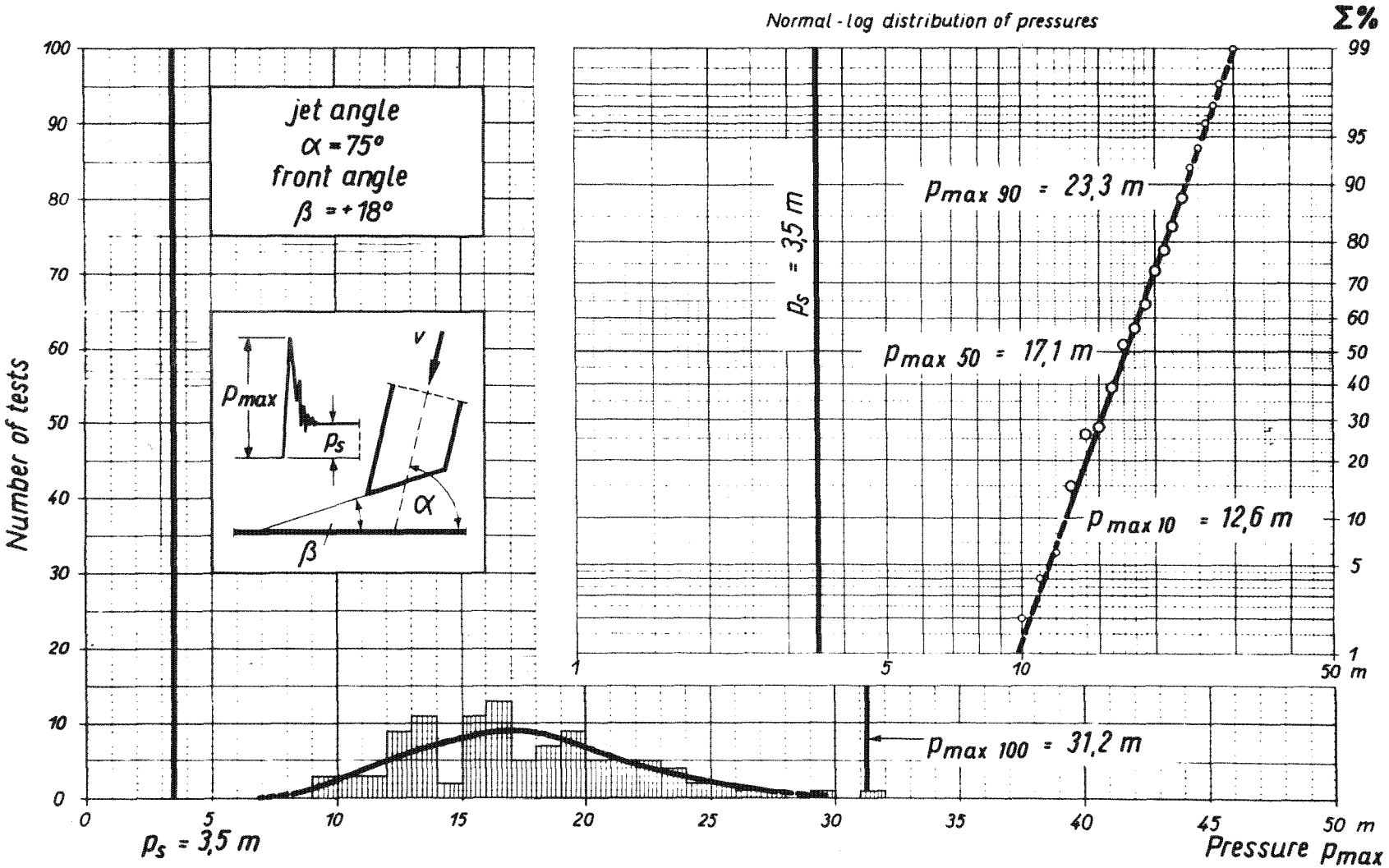

Fig. 6. Frequencies of maximum pressures p_{max}

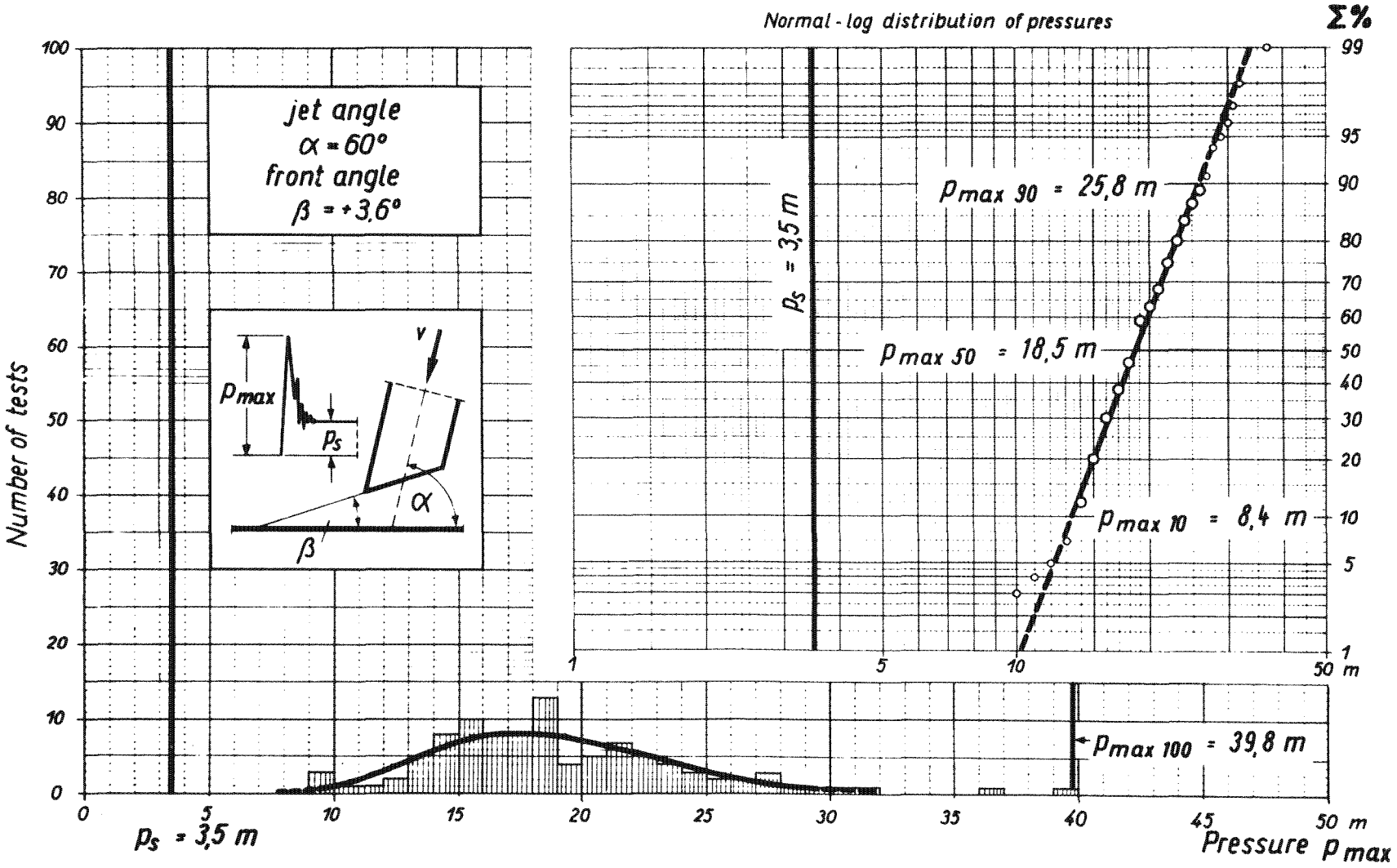

Fig. 7. Frequencies of maximum pressures p_{max}

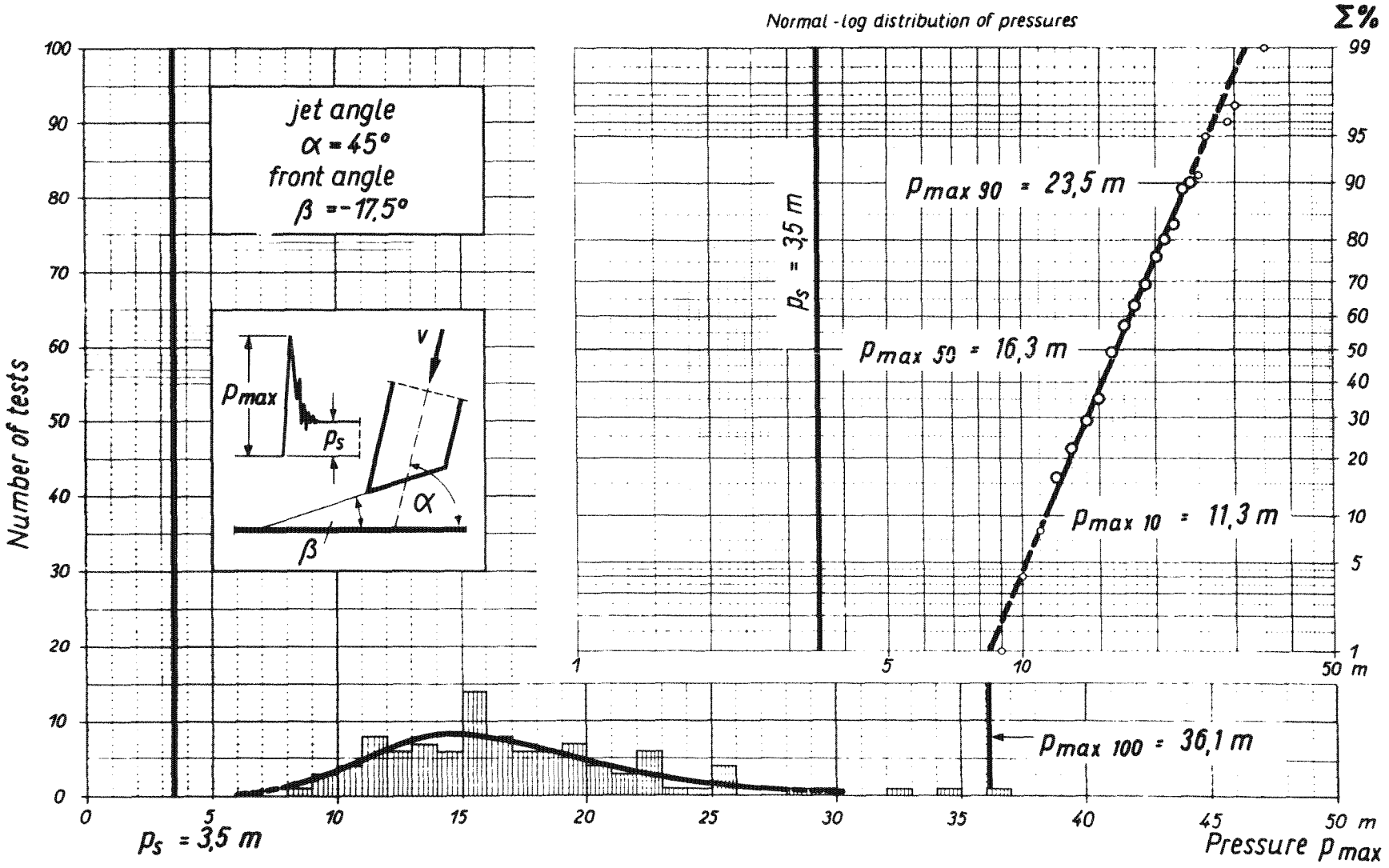

Fig. 8. Frequencies of maximum pressures p_{max}

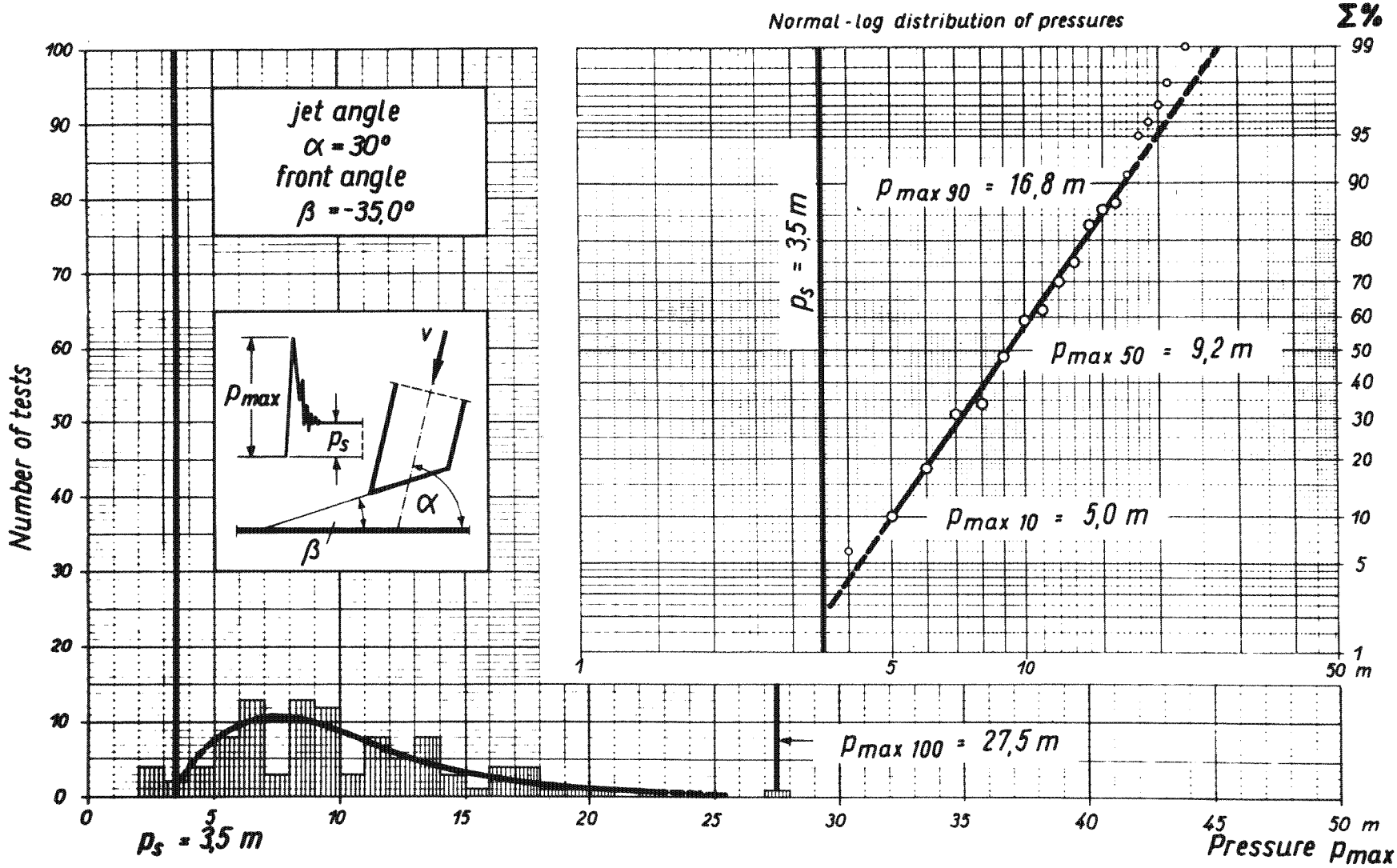

Fig. 9. Frequencies of maximum pressures p_{max}

pressure peaks are more than 10 times higher than p_s (highest pressure was p_{max} = 40.7 m, see Fig. 5).

In Figs. 4 to 9, the original histogram of the frequencies of p_{max} is to be seen as well as the integral function of it on special normal-log function paper. It can be seen from Figs. 4 to 9, that a normal-log distribution is in good agreement with the experimental results; it should be mentioned that the validity of this distribution must be limited by the water hammer pressure $\varrho \cdot v \cdot c$.

In Figs. 4 to 9 the values $p_{max\ 10}$, $p_{max\ 50}$ and $p_{max\ 100}$ are shown; these are the pressures, which are not exceeded by 10, 50 and 90 out of 100 tests; furthermore the highest pressure $p_{max\ 100}$ measured during 100 tests is given on each of Figs. 4 to 9. When these pressures are evaluated by equation (7)

$$p_{max} = \varrho \cdot v \cdot \left(\frac{R}{x}\right)^2 \quad \ldots\ldots\ldots\ldots\ldots\ldots\ldots\ldots\ldots\ldots (7)$$

for the dimensionless number x/R, they can be plotted against the impact velocity v perpendicular to the measuring plane, corresponding to the angle of approach α.

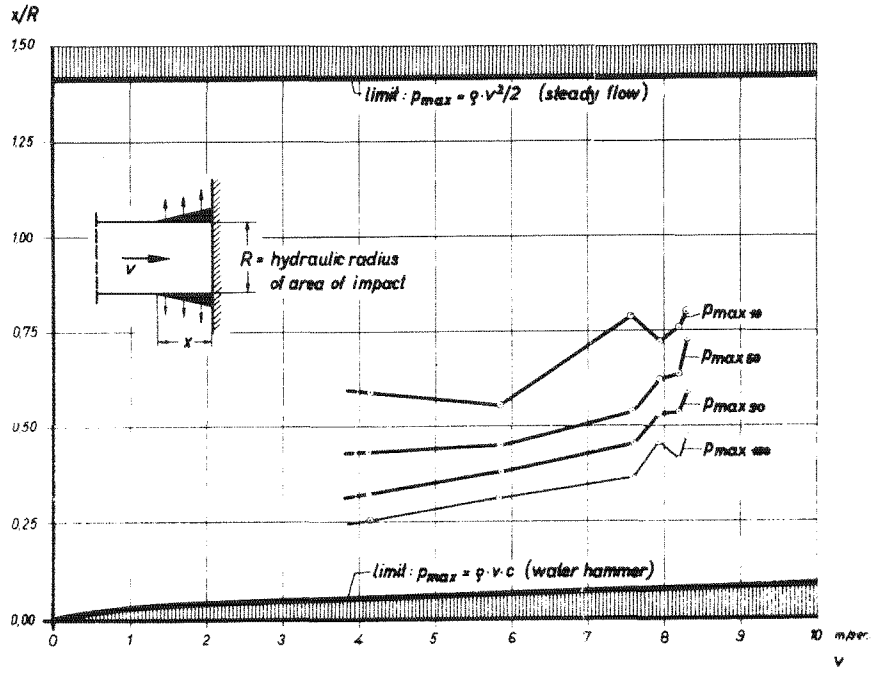

Fig. 10. Expansion factor x/R

The term x/R represents the relation between the length of the volume of expansion and the hydraulic radius R of the impact area; the higher the expansion factor x/R, the lower is the pressure peak. There are two limits for the expansion factor; from equation (8) and (7) follows for the case of steady flow

$$p_s = \varrho \cdot \frac{v^2}{2}; \quad \frac{x}{R} = \sqrt{2} \quad \ldots\ldots\ldots\ldots\ldots\ldots\ldots\ldots \quad (9)$$

and from equation (1) and (7) for the case of water hammer

$$p_{max} = \varrho \cdot v \cdot c; \quad \frac{x}{R} = \sqrt{\frac{v}{c}} \quad \ldots\ldots\ldots\ldots\ldots\ldots\ldots\ldots \quad (10)$$

These limits are also shown in Fig. 10.

It can be seen from Fig. 10, that the expansion factor x/R even for the highest pressures $p_{max\ 100}$ is much higher than for the water hammer, (equation (10)), but also lower than the constant value for steady flow (equation (9)). The hydraulic radius of a jet having a diameter of 200 mm is R = 5 cm; then lie x/R between the extremes .2 and .8 and the length of expansion x between 1 and 4 cm; for the average of pressures $p_{max\ 50}$ x ranges between 2.5 and 3 cm. It must be noted that x is the effective length of expansion only for the time of the maximum of pressure.

As the jet angle α is changing in the 6 series from 90° to 30°, the front angle ß from $+33.8^\circ$ to -35°, it is surprising that the results on Fig. 10 do not differ very much. There is a tendency of increase of x with the velocity v; it may be explained by higher disturbances at the face of the nappe with higher velocities.

Further experiments were conducted in order to study the effect of a water layer on the measuring area; this is the condition when a plunging breaker falls into the backrush water of the foregoing wave. In these experiments only one pressure cell was used in the center of the jet; the angle of approach was 90°.

As shown in Figs. 11 to 13, for 3 velocities (5.8 m/sec, 8.3 m/sec and 10.4 m/sec corresponding to steady flow pressures p_s of 1.7 m, 3.5 m and 5.5 m) the pressure distribution for 100 tests were compared for different depths of water on the (horizontal) impact area. It can be seen that even a thin layer of water is capable to give a high damping effect on the pressure maxima;

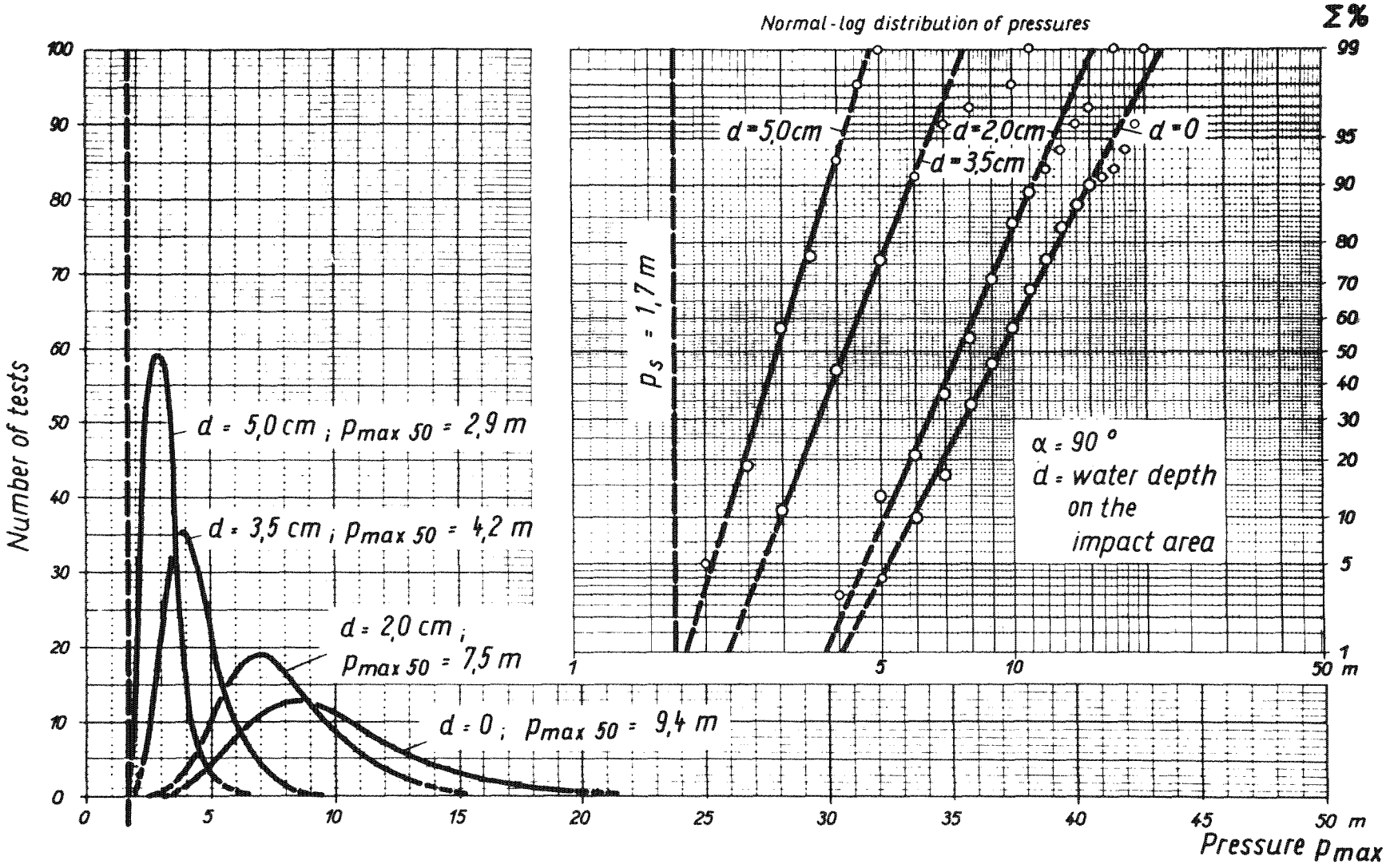

Fig. 11. Damping effect of water on the impact area

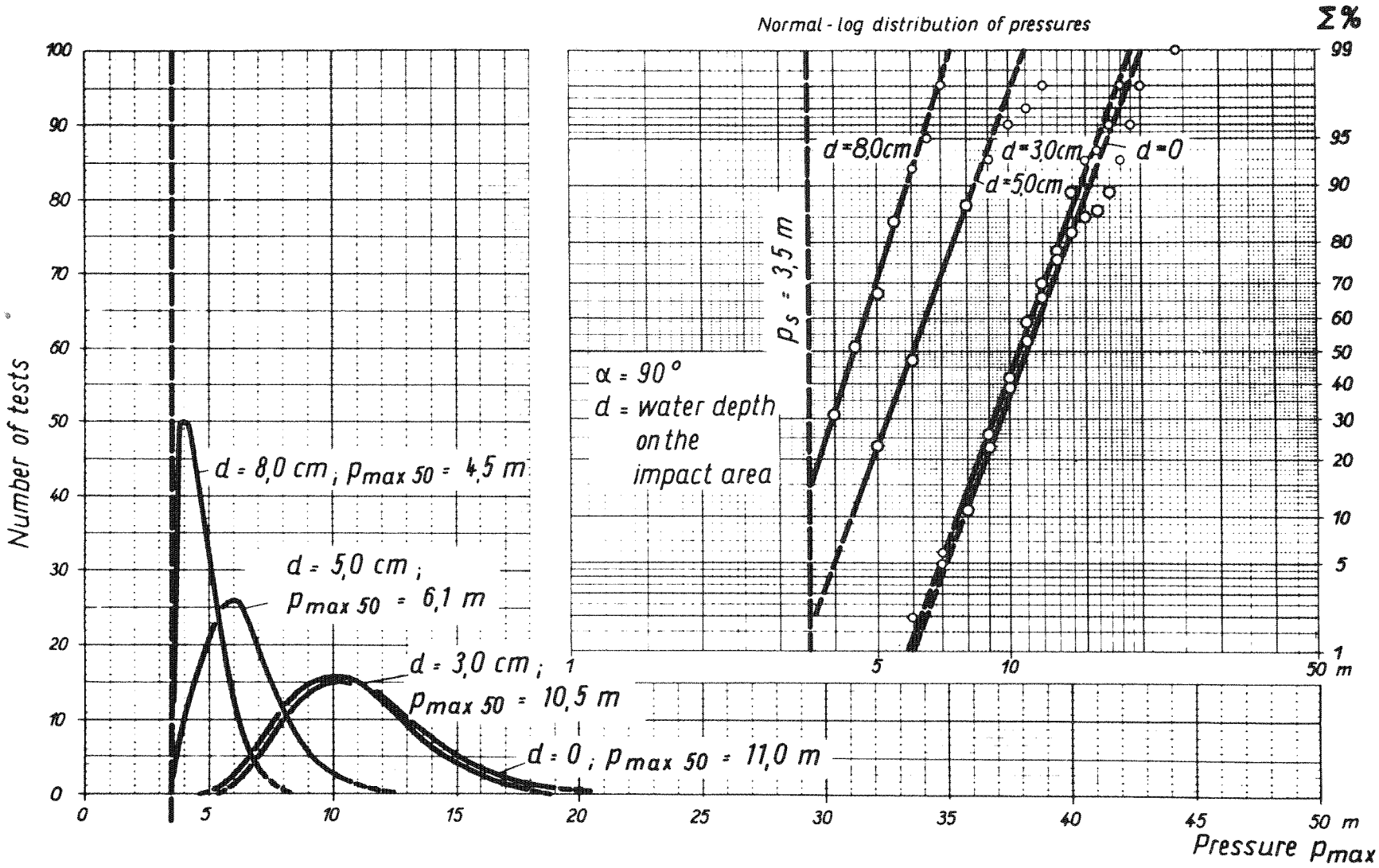

Fig.12. Damping effect of water on the impact area

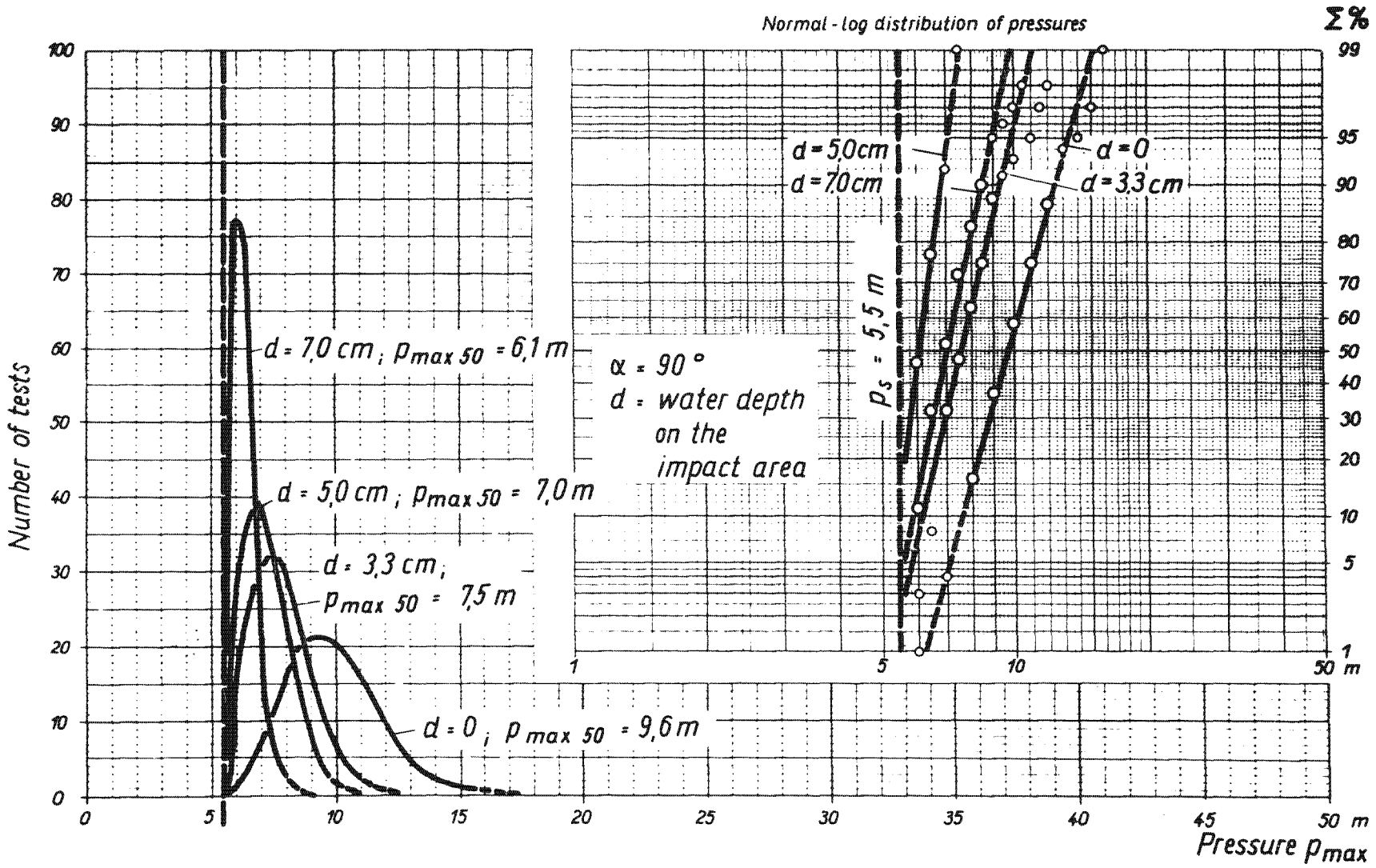

Fig. 13. Damping effect of water on the impact area

for water depths d more than 5 cm the higher pressures are reduced nearly completely.

That agrees with the results shown in Fig. 10; the length of the compressed volume of water and air is in the order of this water depth, therefore the pressure rise does not come till to the bottom formed by the measuring area.

Conspicuous is the fact that for d = v the median $p_{max\ 50}$ is not increasing with velocity; the distribution becomes more uniform for the upper velocities. Because in these series only one pressure cell was used, a direct comparison with the results of Figs. 4 to 9 is not possible, but it agrees with the tendency of x/R versus v in Fig. 10.

4. DISCUSSION OF THE RESULTS

For application to the problems of wave attack, the test material was evaluated in a previous paper (FÜHRBÖTER (4)) into a semi-empirical formula derived from equation (5)

** $$p_{max} = \varrho \cdot v \cdot c \cdot \sqrt[3]{\frac{c}{v} \cdot \delta} \quad \ldots\ldots\ldots\ldots\ldots\ldots \quad (11)$$

with the dimensionless impact-number

$$\delta = \left(\frac{E_a}{E} \cdot \frac{R}{D}\right)^{\frac{2}{3}} \quad \ldots\ldots\ldots\ldots\ldots\ldots\ldots\ldots \quad (12)$$

which was found from the tests to be for $p_{max\ 50}$

$$\delta_{50} = 0.00245 \quad \ldots\ldots\ldots\ldots\ldots\ldots\ldots\ldots \quad (13)$$

with the relations corresponding to the normal-log distribution of p_{max}

$$p_{max\ 10} = 0.65 \cdot p_{max\ 50}$$
$$p_{max\ 50} = 1.00 \cdot p_{max\ 50}$$
$$p_{max\ 90} = 1.5 \cdot p_{max\ 50}$$
$$p_{max\ 99} = 2.1 \cdot p_{max\ 50}$$
$$p_{max\ 99.9} = 2.7 \cdot p_{max\ 50}$$

The time of pressure rise t_1 is given by

$$t_1 = \frac{R}{\sqrt[3]{v \cdot c^2 \cdot \sqrt{\delta}}} \quad \ldots\ldots\ldots\ldots\ldots\ldots \quad (15)$$

In this solution all the results of the 600 tests given in Figs. 4 to 9 are utilized.

Here, only the physical aspect of the results shall be taken into account, which is given by the fact, that from all tests till velocities up to 8.3 m/sec it was found, that the length of expansion (in axis of the jet) was of the same order of of magnitude of R:

$$x \sim R$$

with a tendency of increase for higher values of v.

NAGAI (9) found in his comprehensive tests in model wave tanks a length of 3 to 5 cm of water column which could be related by momentum equation to the shock pressure; this is in agreement with considerations of BAGNOLD (2) who found the length of the participating volume to be about .2 H_B; for waves with H_B of 20 cm therefore about 4 cm. In the tests of the FRANZIUS-INSTITUT the corresponding length x - here defined as the length of the expansion area A_e - also lies in the range between 1 and 4 cm from Fig. 10 with R = 5 cm.

It shall be mentioned here, that the hydraulic radius of impact areas of breaking waves is of the order of half the breaker height H_B. For model waves about 20 cm high the hydraulic radius is not different very much from R = 5 cm in the tests of the FRANZIUS-INSTITUT.

A simple explanation for the fact

$$x \sim R$$

can be given by Fig. 1. Because of the high velocity of sound c in water (compared with v), a build-up of pressure only can occur in a zone of a length x in the order of magnitude like R, because for longer distances from the wall the side expansion effect gives

a pressure about 0 inside the jet during all phases of impact.

Contrary to the theory of NAGAI (9), also with the effect of expansion a water hammer pressure $\varrho \cdot v \cdot c$ would occur, when only the elasticity of water would govern the impact process; but it would appear only for a very short time in the order of $t_1 = R/c$ due to the beginning of expansion.

For the idealized case of a complete parallel front of the nappe to the wall, it can be shown, that the escaping of air out of the volume between the approaching front and the wall is limited by the velocity of sound in air c_a. After arriving to a certain distance from the wall, the escaping velocity of air v_a becomes equal c_a and remains constant for the last time till to the contact of the front of the nappe with the wall. From this idealized model of the process, it follows that a volume of air (under atmospheric pressure)

$$D \sim \frac{R}{2} \cdot \frac{v}{c_a} \quad \ldots\ldots\ldots\ldots\ldots\ldots\ldots\ldots \quad (16)$$

must be included between the (parallel) front of the nappe and the wall.

For R = 5 cm, v = 8.3 m/sec and c_a = 331.6 m/sec equation (16) gives a value of .0012 m or 1.2 mm.

Because of irregularities and disturbances in the front of the jet, it may happen, that more air can escape than from the idealized case of a parallel front; also in opposite direction more air could be entrained by large cavities in the front.

This content of air of equation (16) seems to be very small, but taking into account the relation of elasticities or compressibilities of water and air given by equation (2)

$$\frac{E}{E_a} = 15500 \quad \ldots\ldots\ldots\ldots\ldots\ldots\ldots\ldots \quad (2)$$

it can be shown that this content of air in the compressed volume of the length x is able to explain the damping of water hammer pressures $\varrho \cdot v \cdot c$ to the values of observed shock pressures:

The relation between the compression of the volume of the length x may be related (neglecting the expansion volume) directly to the pressures in it, that is

$$\frac{\frac{A(x-D)}{E} + \frac{A \cdot D}{E_a}}{\frac{A \cdot x}{E}} = \frac{\varrho \cdot v \cdot c}{p_{max}} \quad \text{or}$$

$$p_{max} = \frac{1}{1+(\frac{E}{E_a} - 1) \cdot \frac{D}{x}} \cdot \varrho \cdot v \cdot c \qquad \text{.....(17)}$$

**

Evaluating the pressures $p_{max\ 10}$, $p_{max\ 50}$, $p_{max\ 90}$ and $p_{max\ 100}$ on Figs. 4 to 9 by equation (17) with equation (2), Fig. 14 gives the results for the dimensionless ratio D/x between the thickness D of the air cushion and the length of expansion x.

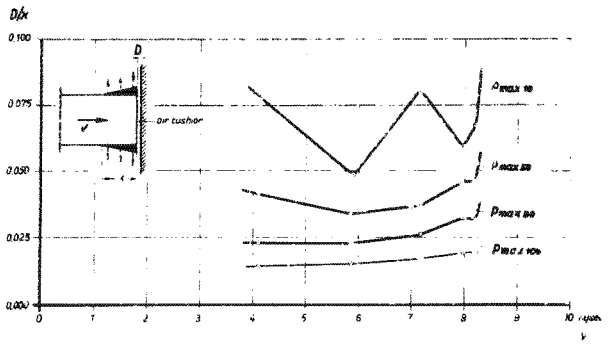

Fig. 14. Air content/expansion length = D/x

From Fig. 10, for the pressure $p_{max\ 100}$, x was found about .5 R = 2.5 cm; with D/x about .04 to .05 from Fig. 14 it can be seen that a thickness D is necessary of

$$D \sim 1 \text{ mm for } p_{max\ 50}$$

in order to explain the relation between observed shock pressure and water hammer pressure; for the highest observed pressures from 100 tests it gives with x/R about .3 from Fig. 10 and D/x about .02 from Fig. 14

$$D \sim .3 \text{ mm for } p_{max\ 100}.$$

Here it is to be taken into consideration, that the factor of equation (2) is variable and decreases with the adiabatic rise of pressure. So equation (17) can only give an approximate approach, but there is a good agreement in the order of magnitude.

Fig. 10 shows for the equation (7) with $p_{max} = p_{max}(v^2)$ an increase of the values of x/R with v according to an increase of the pressure with a lower power of v than 2. From Fig. 14 it can be seen, that also the values of D/x indicate a slight increase with v; that means that the rise of peak pressure is even lower than the power 1 of v (equation (17)). The range of observation is too small to give a clear relation here; from both Fig. 10 (equation (7)) and Fig. 14 (equation (17)) can be seen that the scatter of results by stochastic effects is much higher than the dependence from v. It seems certain that there is also a correlation between x and D as mentioned before, as a high D also may give a higher value of x; by the superposition of the stochastic processes in both, it is not possible here to seperate them. Because the stochastic variable x in equation (7) as well as the stochastic variable D in equation (17) are in the denominator, the always stated normal-log distribution of p_{max} can be explained.

It seems to be sure that the shock pressures do not follow the law of FROUDE as already stated by ALLEN (1), BAGNOLD (2), JOHNSON (6) and MINIKIN (8); RICHERT (10) recently gives a theoretical approach for the scale-up of shock pressures in models; more experimental data are necessary also for this formula.

Because the surface tension of the water is the same in the model as in nature, it is to be expected that scale effects occur in a manner that small model waves with considerably smooth fronts have lower air content than larger waves in nature.

Especially for high impact velocities, there is a lack of information about the shock pressures produced by them. The present paper will give a contribution to this problem.

5. LIST OF SYMBOLS

A	=	Area of impact on the wall
A_e	=	Area of expansion at the sides of the jet
D	=	air content, represented by an uniform thickness on the area A
E	=	elasticity of water = $\varrho \cdot c^2$
E_a	=	elasticity of air = $\varrho_a \cdot c_a^2$
H_B	=	height of breaker
Q	=	inflow of the jet = $A \cdot v$
Q_e	=	outflow through the area of expansion $A_e = A_e \cdot v_e$
R	=	A/U = hydraulic radius of impact area
U	=	circumference of the area of impact
c	=	velocity of sound in water = 1485 m/sec for 0° C and atmospheric pressure
c_a	=	velocity of sound in air = 331.6 m/sec for 0° C and atmospheric pressure
d	=	water depth on the measuring area
g	=	gravitational acceleration = 9.81 m/sec^2
p	=	pressure
p_{max}	=	maximum of pressure during impact
$p_{max\ 10}$	=	pressure not exceeded by 10 % from 100 tests
$p_{max\ 50}$	=	pressure not exceeded by 50 % from 100 tests
$p_{max\ 90}$	=	pressure not exceeded by 90 % from 100 tests
$p_{max\ 100}$	=	highest pressure measured during 100 tests
p_s	=	maximum pressure of steady flow with the velocity v = $\varrho \cdot \frac{v^2}{2}$
t_1	=	time of pressure rise from p=o to $p=p_{max}$
t_2	=	time of pressure drop from $p=p_{max}$ to $p=p_s$
t_s	=	$t_1 + t_2$ = total duration of impact
v	=	velocity of impact, perpendicular to the measuring plane
v_e	=	velocity of water due to expansion on the sides of the jet
v_a	=	escaping velocity of air between the front of the jet and the wall
x	=	length of expansion area in axis of the jet
α	=	jet angle or angle of approach (Fig. 3)
β	=	front angle (Fig. 3)
δ	=	dimensionless number of impact given by equation (12)
ϱ	=	density of water
ϱ_a	=	density of air

6. REFERENCES

1. ALLEN, J. — Scale Models in Hydraulic Engineering
Longmans, Green and Co.,
London 1947

2. BAGNOLD, R.A. — Interim Report on Wave Research
Journal Inst.Civ.Eng. Vol. 12, 1938/1939

3. DENNY, D.F. — Further Experiments on Waves Pressures
Journal Inst.Civ.Eng. Vol. 35, 1951

4. FÜHRBÖTER, A. — Der Druckschlag durch Brecher auf Deichböschungen
Mitt. Franzius-Institut Heft 28, 1966

5. GAILLARD, D.D. — Wave Action
Eng. School Fort Belvoir, Virgina 1904

6. JOHNSON, J.W. — Deficiencies in Research on Gravity Surface Waves
Council on Wave Research
Eng.Found., 1961

7. von KARMAN, Th. — The Impact of Seaplanes during Landing
N.A.C.A. TN 321, 1929

8. MINIKIN — Wind, Waves and Maritime Structures
Charles Griffin a.Co.Ltd., London 1950

9. NAGAI — Shock Pressures exerted by Breaking Waves on Breakwaters
Transact. ASCE Vol. 126 part IV, 1961

10. RICHERT, G. — Model Law for Shock Pressure against Breakwaters
Coastal Engineering Conference London 1968